READ 2024
RESEARCH & EDUCATION IN AIRCRAFT DESIGN
WARSAW, POLAND | 6-8 NOVEMBER 2024

DETERMINATION OF UAV LOADS BASED ON FLIGHT SIMULATION RESULTS

Jakub Kuliberda [1] & Agnieszka Kwiek[2]

[1]Warsaw University of Technology, Faculty of Power and Aeronautical Engineering
[2]Warsaw University of Technology, Faculty of Power and Aeronautical Engineering, Institute of Aeronautics and Applied Mechanics

Abstract

This study was conducted for a small UAV, designed in a tailless configuration, to define loads limit through flight simulations. Analyses presented in this paper are restricted to the longitudinal motion, which is controlled by elevons. Aerodynamic analyses were carried out with the use of MGAERO. Obtained characteristics were used in creation of the simulation model. The UAV simulations were performed with the use of the Simulation and Dynamic Stability Analysis (SDSA) package and MATLAB Simulink. SDSA can simulate the aircraft as a rigid body with 6 degrees of freedom, including response to control. To collect the data a few manoeuvres were tested, each of them was commanded by a step or doublet elevons deflection. While in case of the gust loads, the “1-cos” wind shape model was assumed. The results revealed that the use of a flight envelope and manoeuvring loads regarding horizontal control surfaces, included in classic aircraft regulation, would overestimate the maximum loads.

Keywords: flight simulations, response to control, loads, unconventional configuration, UAV

1. Introduction

A typical approach to defining loads for manned civil aircraft consists in calculations of load envelope, which is described in regulations appropriate for the aircraft type. In case of a small UAV, the regulations do not specify mathematical model to calculate the load envelope. In the military domain, for a UAV heavier than 150kg, NATO standards are recommended [13], but those regulations are based on manned EASA Certification Specification CS23. If a small UAV is going to be designed in classical configurations, adaptation of manned regulations can be a feasible solution. But this approach might rise issues if an unconventional UAV is designed, especially one that is flying with a relatively high speed. This paper addresses this problem by the use of flight simulation to define the limit loads. This study was conducted for a small UAV testing platform designed in a tailless configuration. At the beginning of the paper a presentation of the UAV is included. Next, description of the methodology is provided that includes an elucidation of manoeuvres selected to determine loads. The next section is dedicated to description of MGAERO software and Simulation and Dynamic Stability Analysis package, which were respectively used in aerodynamics computation and flight simulations. Next, the results are presented, and key findings are encapsulated.

2. State of the art

A few tools for preliminary aircraft design can be listed, like: Computerized Environment for Aircraft Synthesis and Integrated Optimization Method (CEASIOM) [15] and [16], aircraft conceptual design and analysis system (ACDAS) [17], a conceptual level aircraft design environment SUAVE [1], Advanced Aircraft Analysis by DAR Corporation [1], and Flight Optimization System (FLOPS) [5] developed by NASA, more examples of tool can be found in [17]. Some of them are available for free while others required buying a licence. Tools with different fidelity are available and covering a different scope of design process. But in terms of load envelope, it is always estimated based on the regulations. None of those software implemented flight simulations to assess the loads on the preliminary stage of design. On the other hand, in case of classic aircraft configuration, the aircraft regulation covers all necessary aspects and making flight simulations on this stage of design is unnecessary. However, in case of unconventional design, some of assumptions might not be appropriate. Load determination due to wind guest can be addressed by implementation of cosine model of wind [3]. This approach is common when an aeroelasticity effects are modelled [18]. In the CS 23 regulations a simplified model of wind guest is assumed, quasi static model [14] which is known as Pratt's formula.

As it was mentioned, the classic approach of loads determination consists in creation of the load envelope based on the aircraft regulations. The key parameter in the load envelope estimation is the maximum lift coefficient, in case of the classic configuration, the impact of the elevator deflection on lift coefficient is negligible. In tailless configuration, in contrast to a conventional one, wing and horizontal control surfaces are not separated physically nor functionally. If resulting pitching moment is to remain zero, shorter arm $(x_E - x_{CG})$ of force L_E on elevator in Figure 1, while maintaining other values constant, necessitate greater value of that force.

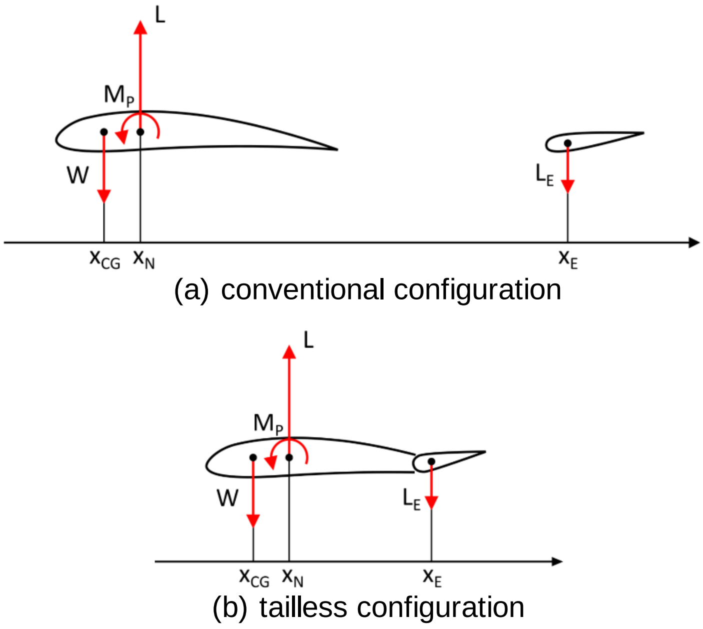

Figure 1 – Schematic representation of forces and moments on aerodynamic surfaces

Since it acts in opposite direction than lift L, resultant lift force has lower value than for conventional configuration at equal AoA. Moreover, maximum AoA and maximum lift coefficient $C_{L\,max}$ are limited by available elevon deflection. Lift coefficient versus angle of attack curves for clean wing and wing with elevons deflected for trimmed flight presented in Figure 2 visualize these effects. Thereby calculations based on regulations were carried out for C_L in trimmed conditions.

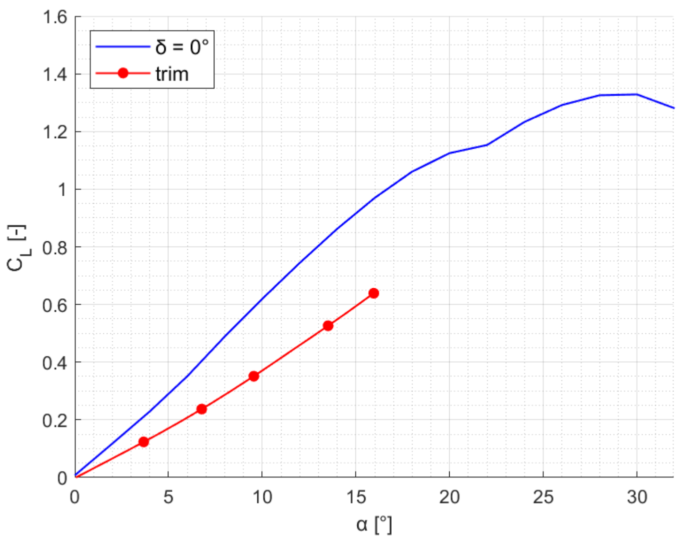

Figure 2 – C_L versus AoA for untrimmed and trimmed elevon deflection

3. UAV model

This research was carried out for a UAV design in unconventional configuration. The tailless configuration with side plates mounted on the wing tip was selected. The design was originated by the concept of the rocket plane for suborbital flights [3] and [6]. But was converted into UAV technology testing platform, so the fuselage was redesigned to get smaller base drag. The fuselage shape is axially symmetric which allows for easy integration of the different kinds of engines. Moreover, the LEX and side plates were modified because the high manoeuvre capabilities are not required in this project. Pitch and roll control is provided by the elevons while the yaw channel control is ensured by the rudders located on the side plates. The layout of the UAV is presented in Figure 3, the elevons are highlighted in dark blue. It was assumed that maximum take-off mass of the UAV is less than 15kg and maximum design speed is less than 500km/h. All presented result were obtained for this maximum mass.

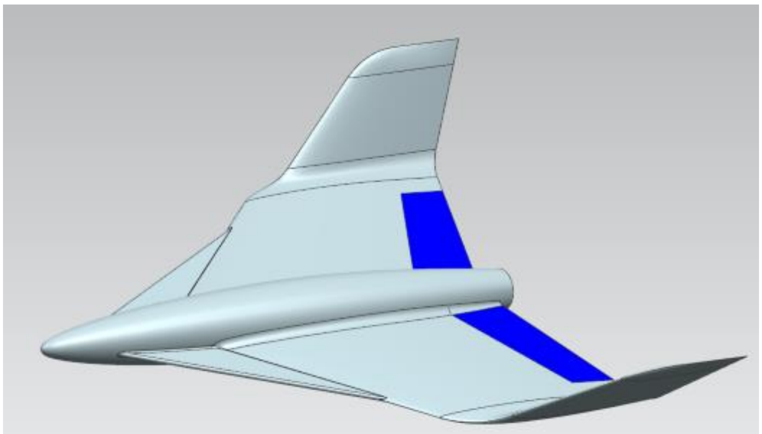

Figure 3 – UAV layout with highlighted elevons

Experimental tests carried out with the use of this UAV are planned, so the load determinations are necessary to design the internal structure of the aircraft. Due to relatively small size and great speed the determination of the loads is a key factor for success. The experiment assumes that aircraft is accelerated to high speed and then performs flight in a glide mode, so the presented analysis focus on scenario when engine is off. During the acceleration phase the critical loads came from the thrust and mainly act in the longitudinal axis.

4. Methodology

To address the research question both regulations and simulation technique were used. In terms of the regulations, CS 23 was assumed. The goal of the simulations was to determine loads due to manoeuvres and due to gusts. To determine those loads, the set of the manoeuvres was planned. The simulation scenario was executed with the following assumption, that the starting conditions of each unpowered manoeuvre, including elevons deflection, assure moments and forces equilibrium. Selection of manoeuvres was imposed by the capabilities of the software which is explained in section 5.2. Following manoeuvres were investigated:

Manoeuvre 1: Pull-up (Figure 4):

- single step negative deflection by $\Delta\delta$, elevons deflect upwards and aircraft reaches greater angles of attack than while maintaining moment equilibrium.

This manoeuvre allows for investigation of dynamically achieved load factors.

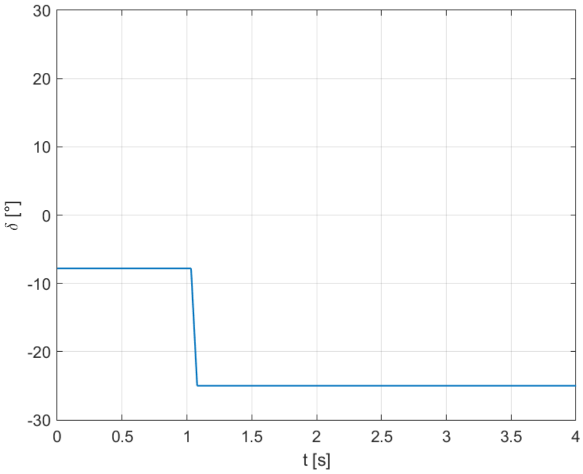

Figure 4 – Exemplary elevon deflection of pull-up manoeuvre

Manoeuvre 2: Push-over (Figure 5):

- single step positive deflection by $\Delta\delta$, elevons deflect downward and aircraft dives
- after specified time Δt elevons return to initial deflection

First deflection allows for investigation of loads generated by sudden change in camber, leading to more extreme instant load factor. Likewise, second deflection, but during non-1g flight.

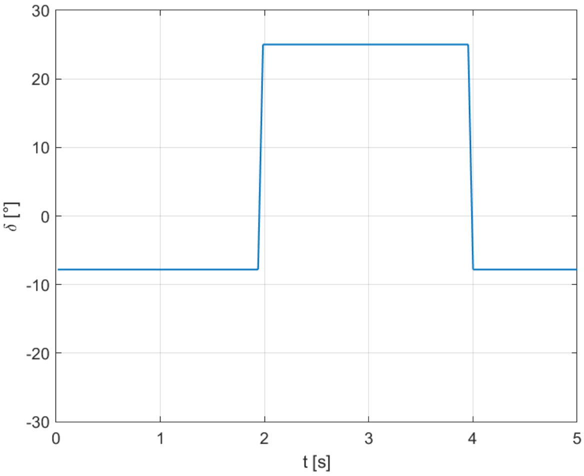

Figure 5 – Exemplary elevon deflection of push-over manoeuvre

Manoeuvre 3: Doublet deflection (Figure 6):

- deflection by $\Delta\delta$ in one direction for time Δt
- followed by deflection by $\Delta\delta$ in opposite direction for time Δt
- elevons return to initial deflection

This manoeuvre was investigated for deflections in both directions and for Δt lower than 1 second. It allows to inspect the interference of load factors resulting from dynamically achieved AoA and sudden elevon deflection. Because starting elevon deflection is non-zero and subsequent deflections are of equal amount $\Delta\delta$, it was not possible to conduct deflections between opposite allowed elevon positions.

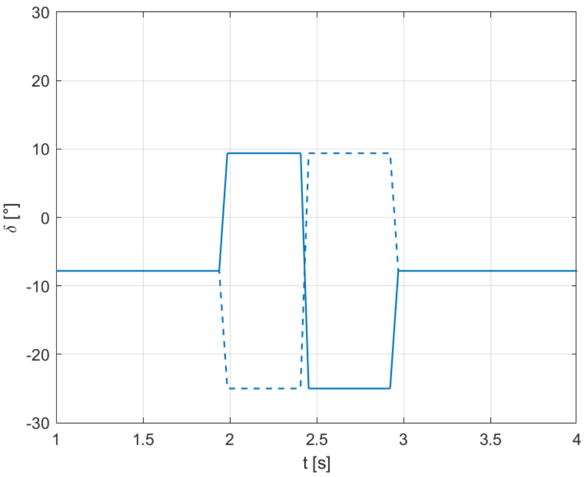

Figure 6 – Exemplary elevon deflection of doublet deflection manoeuvre

5. Numerical model

5.1 Aerodynamics

Due to necessity of taking into account the nonlinear part of aerodynamic characteristics and compressible effect, the software based on the Euler's equations was selected for computations. Considering that the loads must be determined at the preliminary stage of the design, it is a good compromise between the time of the computations and the flow model accuracy [7]. So, the MGAERO software was used to obtain aerodynamic coefficients, stability and control derivatives. This is a commercial CFD software using Euler's equations and multigrid scheme [12]. The numerical model consisted of 42 848 on-body panels and 13 344 418 grid points which created a multigrid structure with 6 levels of blocks.

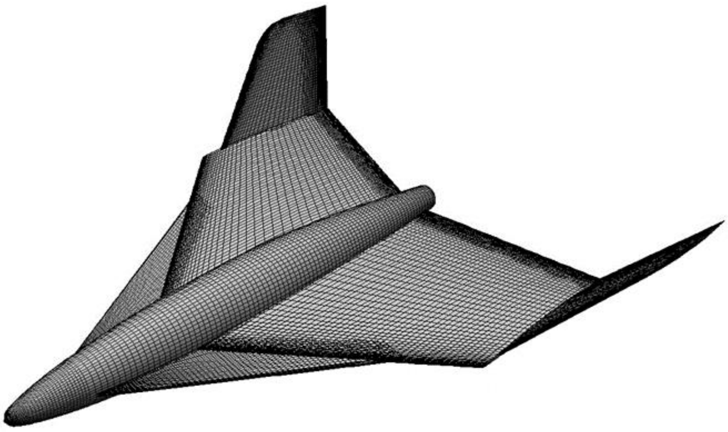

Figure 7 – Numerical model of the UAV – on-body mesh

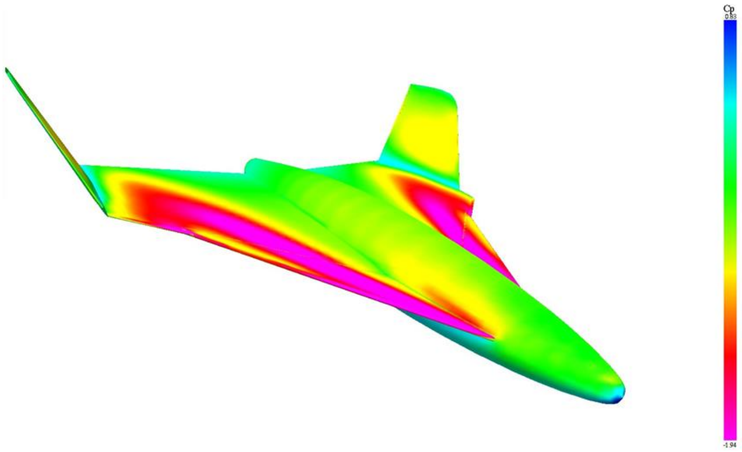

Figure 8 – Exemplary Cp distribution obtained by MGAERO software in case of Ma=0.3 and AoA=18 degrees.

Figure 7 shows the aerodynamic model mesh while the exemplary pressure distribution is presented in Figure 8. Aerodynamic characteristics computed by the MGAERO are presented in Figure 9. The control and stability derivatives were also computed with the use of the MGAERO software. Due to unconventional configuration, derivatives vary with AoA, an example of selected stability derivatives is presented in Figure 10.

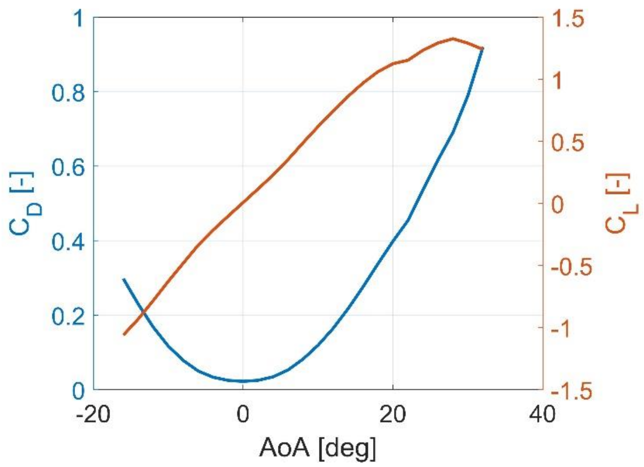

Figure 9 – Lift and drag coefficients versus angle of attack

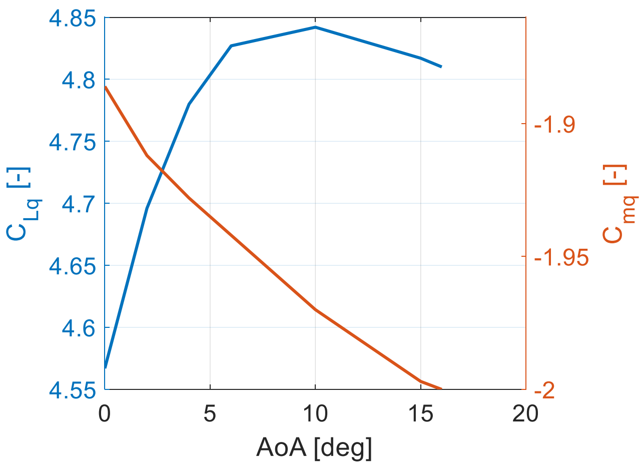

Figure 10 – Derivatives of lift coefficient and pitching moment coefficient with respect to the pitch rate

5.2 Flight dynamics

To predict the aircraft behaviour during the defined manoeuvres, a flight simulation with 3 degrees of freedom was utilised (2 translations and rotation in the pitch axis). The simulations were performed with the use of the Simulation and Dynamic Stability Analysis (SDSA) package [7], [9]. The mathematical model implemented in this package allows for simulations of the aircraft with 6 DoF (3 translations and 3 rotations) as a rigid body under the following assumptions: aerodynamics is quasi-steady [3], deflection of control surfaces do not affect change of the centre of gravity and moment of inertia, no aeroelastic effects are included, atmosphere is calm and modelled in accordance with the ISA. Figure 11 presents a single frame during simulation of pull-up manoeuvre with initial speed of 60 m/s and deflection of 25°.

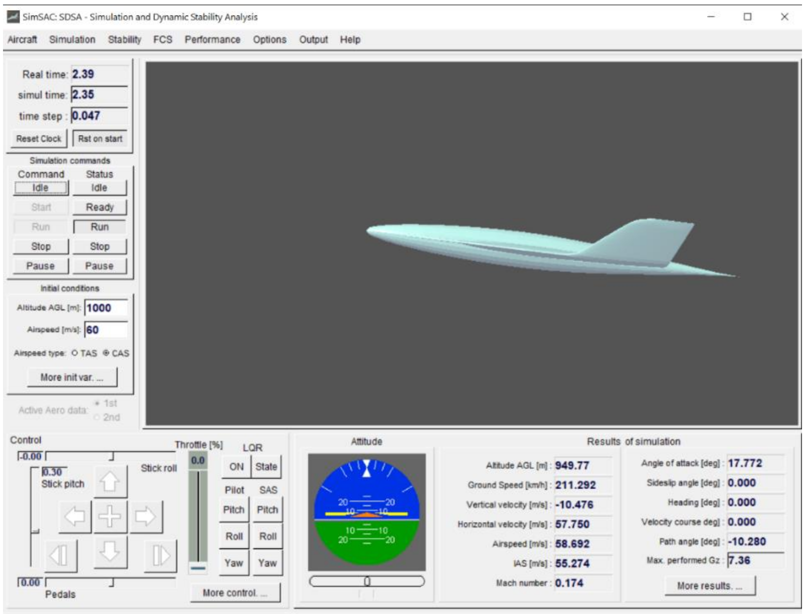

Figure 11 – single frame during simulation of selected manoeuvre

Within the SDSA simulation feature the response of control can be modelled. The software allows for testing one of the following scenario: single step, doublet, and single step with return to the initial deflection of the control surface. Naturally, the selection process of considered manoeuvres took into account limitations of the package. The setup allowing to control the parameters presented in Figure 12 contains, among others, available control types, controlled surfaces and control parameters such as deflection by value $\Delta\delta$ and duration Δt of that deflection.

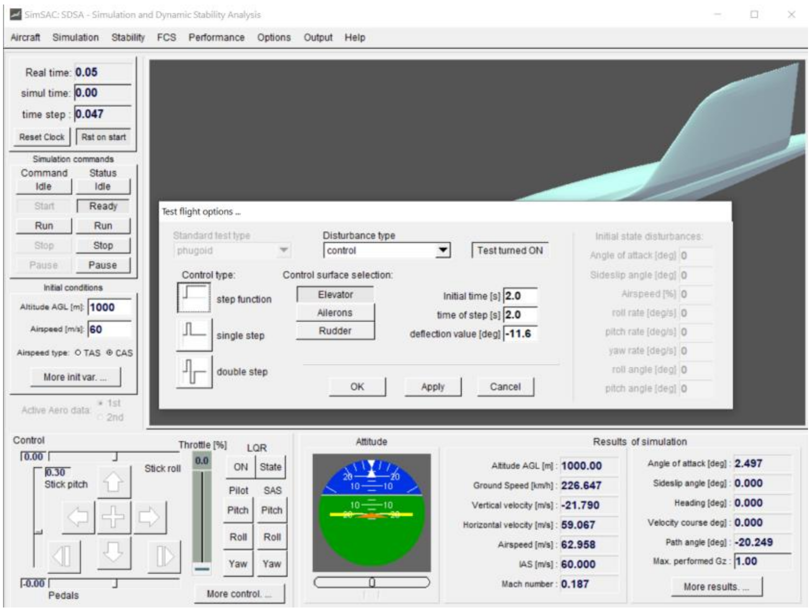

Figure 12 – SDSA parameters setup window picture

Also, in SDSA, a turbulence model is implemented. This feature was used to determine the way the gusts impact. In addition, the second set of simulations were performed to determine the load factor due to gusts. To address this problem, the aircraft flight dynamics model was created in Simulink. The Aerospace Block set was used to create numerical model which includes the Discrete Wind Gust Model [11], which is based on the “1-cos” wind shape model. The same wind model is defined in the CS regulations. The gust shape can be described by equation (1):

$$U = \frac{U_{de}}{2}\left(1 - \cos\frac{2\pi s}{lg}\right) \tag{1}$$

where: U_{de} – the gust velocity, s – distance penetrated into gust, and lg – the gust length.

In case of the CS 23, the gust length is assumed as 25 times mean geometrical chord. So, in this paper, to make the simulation’s results comparable with the regulations, the same gust length was assumed.

6. Results

6.1 Analytical - regulations

Because foreseeable flight conditions do not include intensive negative g manoeuvres, limited lift coefficient has the effect only on curve $V_{S1} - V_A$ of flight envelope. Influence of allowed elevon deflection on load factor for corresponding C_L was investigated. Results presented in Figure 13 show that elevon efficiency drops above $\delta = 20°$. Clean wing without pitching moment equilibrium, represented by dotted line, generates much greater load factors.

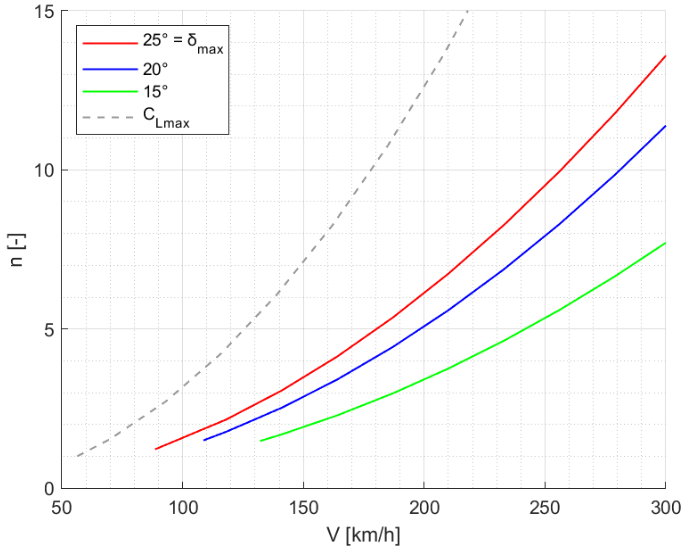

Figure 13 – Loads for different elevon deflections in trimmed conditions as a function of speed, dotted line represents loads for $C_{L\,max}$ of clean wing

Presented aircraft has control surfaces embedded into the wing (elevons), thus their loading resulting from manoeuvring was also investigated. Condition of sudden downward deflection in flight at 1g was chosen because it results in greater load factor than upward deflection. Because this analysis does not account for dynamic effects, following assumptions were made:

- deflection is instantaneous
- aircraft and control surfaces are a rigid body
- aircraft remains in current orientation
- C_L change is instantaneous and depends only on elevon deflection change

This analysis allows for examination of influence of sudden elevon deflection on load factor. Results presented in Figure 14 show that load factor rises proportionally with elevon deflection.

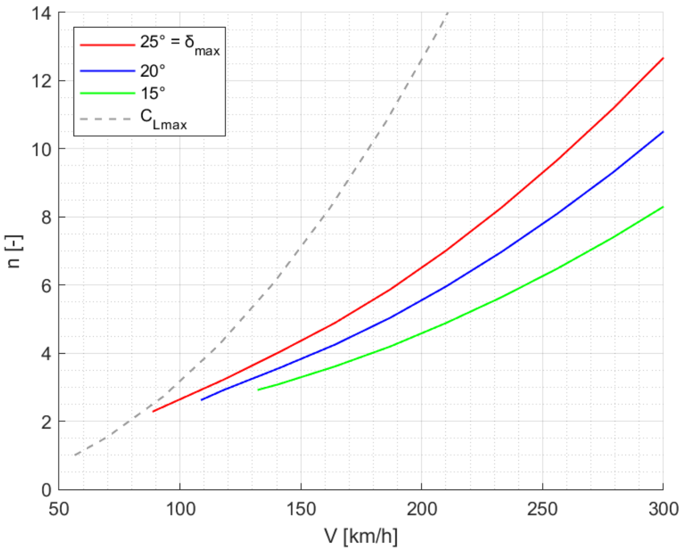

Figure 14 – Loads for different elevon deflections of sudden deflection manoeuvre as a function of speed, dotted line represents loads for $C_{L\,max}$ of a clean wing

Flight envelopes modified to account for trimmed flight conditions are presented in Figure 15. For gust speeds provided in regulations, manoeuvring envelope conditions are far from flight conditions determining structural limits. It is possible to increase default n_{max} significantly without influencing combined envelope.

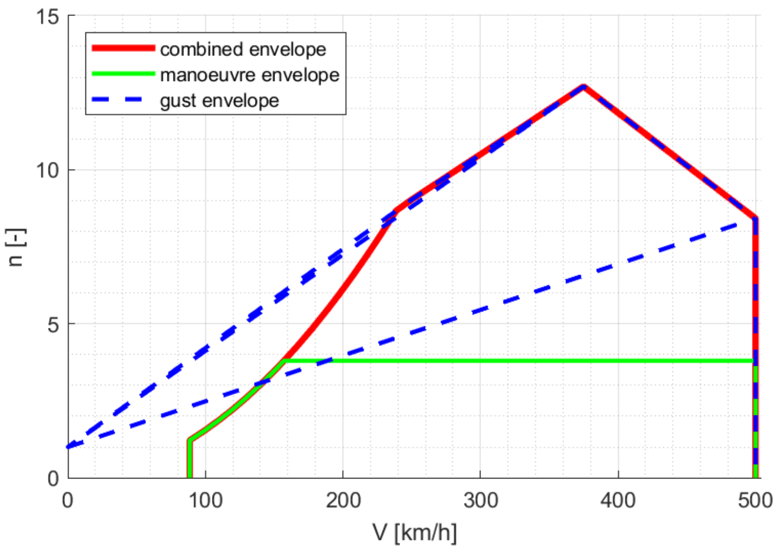

Figure 15 – Subsequent envelopes resulting from modified regulations

6.2 Simulations

Comparison of extreme load factors at their corresponding speeds of analytical calculations and simulations conducted in SDSA are presented in Figure 16.

Figure 17 presents, that load factors in a very aggressive and sudden doublet deflection manoeuvre M3, while 100% greater than during trimmed manoeuvre, are still lower than these resulting from unmodified regulations. However, in such a simple manoeuvre as M1 pull-up, g-forces are greater than these of trimmed manoeuvre according to modified regulations, by less than 20%. Manoeuvre M2 specified by reasonable control input results in intermediate load factors, 30% greater than trimmed ones. Extrapolated M3 and M2 lines appear to cross above stall speed. It results from greater relative $\Delta\delta$ at low speeds for positive deflection during manoeuvre M2, since deflection needed for trimmed flight becomes more negative.

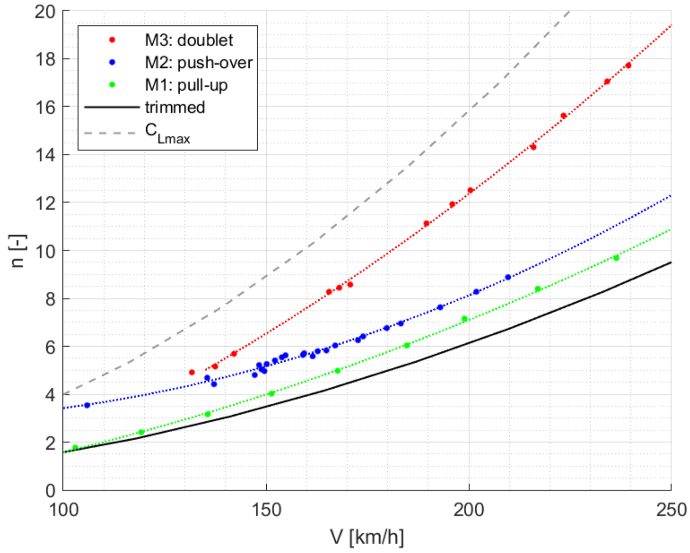

Figure 16 – Load factors as a function of speed for selected manoeuvres

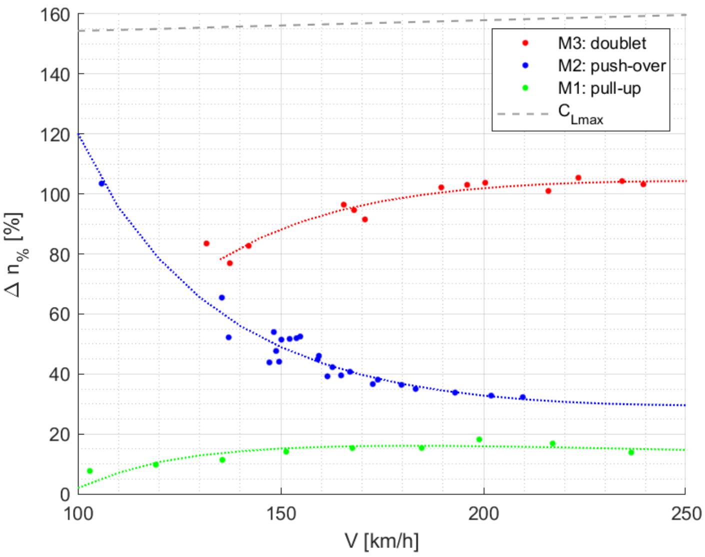

Figure 17 – Relative load factor increase as a function of speed for selected manoeuvres

The next set of results is associated with impact of gusts on the load factor predicted by the Simulink model. Figure 18 shows the comparison of the load factor obtained by analytical method and outcome of the simulation, it can be noticed that simulations resulted in lower values.
Moreover, flight simulations with medium and extreme turbulence were performed with the use of the SDSA package. The maximum angle of attack increment due to gust impact is presented in Figure 19, both simulations and analytical results are compared. Greater increment is associated with greater force which results in greater load factor. In case of the VC, the analytical value is greater than simulation while in case of VD, the trend is opposite.

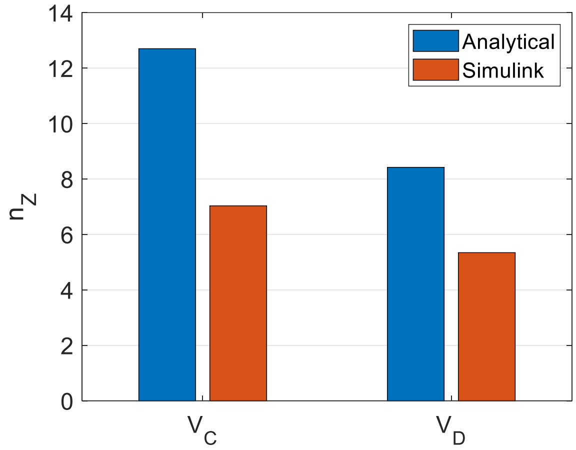

Figure 18 – Comparison of the load factor due to gust in case of analytical calculations and simulation results

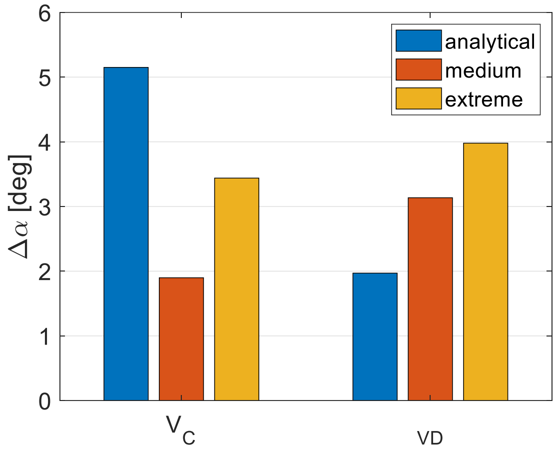

Figure 19 – AoA increment due to gust, obtained by analytical way (regulations) and by SDSA in case of simulation with medium and extreme turbulence atmosphere model.

7. Conclusions

In this paper it was presented, that following regulations would lead to oversized structure designed for much greater loads. Geometry of presented aircraft necessitated alteration of methodology presented in regulations to take into account absence of tail control surfaces and its influence on trimmed flight conditions. Analytically computed load factors proved to be significantly lower than these computed in a standard manner. Load factors achieved during simulations of manoeuvres were obviously greater than these in modified static manoeuvres and for a reasonable manner of manoeuvring they are not greater than 30%, which is significant in comparison to safety factor of 1.5. However, even the greatest achieved g-load values in most extreme manoeuvre were lower than these resulting from unmodified regulations. Gust loads achieved during simulations also proved to be lower than these calculated by methods presented in regulations. Therefore, utilization of advanced methods is crucial in designing light and manoeuvrable aircraft.

8. Contact Author Email Address

Agnieszka Kwiek mailto: agnieszka.kwiek@pw.edu.pl

9. Copyright Statement

References

[1] Advanced Aircraft Analysis - Aeronautical Software - https://www.darcorp.com/advanced-aircraft-analysis-software/

[2] Botero, E.M., Wendorff, A., MacDonald, T., Variyar, A., Vegh, J.M., Lukaczyk, T.W., Alonso, J.J., Orra, T.H. and da Silva, C.I. SUAVE: an open-source environment for conceptual vehicle design and optimization, *54th AIAA Aerospace Sciences Meeting*, Aerospace Research Central, San Diego, CA, 2016

[3] Cook, M. Flight Dynamics Principles: A Linear Systems Approach to Aircraft Stability and Control, 3rd ed.; Butterworth-Heinemann: Oxford, UK, 2013

[4] Figat M., Galiński C., Kwiek A. (2012), Modular Aeroplane System. A Concept and Initial Investigation, Proceeding of the 28th Congress of the International Council of the Aeronautical Sciences, Brisbane, Paper ICAS 2012-1.3.2

[5] Flight Optimization System (FLOPS) software - https://software.nasa.gov/software/LAR-18934-1

[6] Galiński C., Goetzendorf-Grabowski T., Mieszalski D., Stefanek Ł., (2007), A concept of two-staged spaceplane for suborbital tourism, Transactions of the Institute of Aviation, No. 4 (191), pp.33-42

[7] Goetzendorf-Grabowski T, Kwiek A. Study of the Impact of Aerodynamic Model Fidelity on the Flight Characteristics of Unconventional Aircraft. *Applied Sciences*. 2023; 13(22):12522. https://doi.org/10.3390/app132212522

[8] Goetzendorf-Grabowski T., Mieszalski D., and Marcinkiewicz E. Stability analysis using SDSA tool. *Progress in Aerospace Sciences*, 47(8):636–646, November 2011 https://doi.org/10.1016/j.paerosci.2011.08.007

[9] Goetzendorf-Grabowski T. SDSA - Simulation and Dynamic Stability Analysis application. https://www.meil.pw.edu.pl/add/ADD/Teaching/Software/SDSA , 2020. (Accessed on 08/07/2024)

[10]MGAERO A Cartesian Multigrid Euler Code for flow Around Arbitrary Configurations - User's Manual Version 3.1.4, 2001.

[11]MATLAB Simulink – discrete wind gust model https://ch.mathworks.com/help/aeroblks/discretewindgustmodel.html

[12] Mavriplis D. J. Three-dimensional unstructured multigrid for the Euler equations. *AIAA Journal*, 30(7), pp.1753–1761, 1992

[13]NATO Standard AEP-4671 Unmanned Aircraft Systems Airworthiness Requirements (Usar) Edition B Version 1, April 2019

[14]Pratt K G, and Walker W G, A revised gust-load formula and a re-evaluation of V-G data taken on civil transport airplanes from 1933 to 1950. National Advisory Committee for Aeronautics. Langley Aeronautical Lab., Langley Field, VA, Technical Report NACA-TR-1206, 1953.

[15]Rizzi, A. Modeling and simulating aircraft stability and control – the SimSAC project, *Progress in Aerospace Sciences*, Vol. 47 No. 8, pp. 573-588, 2011

[16]R. von Kaenel, A. Rizzi, J. Oppelstrup, T. Goetzendorf-Grabowski, M. Ghoreyshi, L. Cavagna, A. Bérard, CEASIOM: Simulating Stability & Control with CFD/CSM in Aircraft Conceptual Design, Proceedings of 26th International Congress of the Aeronautical Sciences, ISBN 0-9533991-9-2, 2008

[17]Ünal, N., Öz, Y. and Oktay, T., "Conceptual design modeling by the novel aircraft conceptual design and analysis system (ACDAS)", Aircraft Engineering and Aerospace Technology, Vol. 95 No. 5, pp. 799-813, 2023, https://doi.org/10.1108/AEAT-02-2022-0056

[18] Voß A., Klimmek A. Aeroelastic Modeling, Loads Analysis and Structural Design of a Fighter Aircraft, *International Council of the Aeronautical Sciences*, Stockholm, Sweden (2022)